Süleyman Demirel Üniversitesi
Fen Bilimleri Enstitüsü Dergisi
Cilt 29, Sayı 1, 44-53, 2025

Süleyman Demirel University
Journal of Natural and Applied Sciences
Volume 29, Issue 1, 44-53, 2025

DOI: 10.19113/sdufenbed.1599212

Novel Furan-Imine Substituted Zinc Phthalocyanine with Increased Singlet Oxygen Formation by Sono-Photochemical Method

Gürkan KARANLIK[*1,2]

[1]Yildiz Technical University, Faculty of Chemical and Metallurgical Engineering, Department of Bioengineering, 34220, Istanbul, Turkey

[2]Health Biotechnology Joint Research and Application Center of Excellence, 34220, Istanbul, Turkey

(Alınış / Received: 10.12.2024, Kabul / Accepted: 12.02.2025, Online Yayınlanma/ Published Online: 25.04.2025)

Keywords
Photodynamic therapy,
Sono-photodynamic therapy,
Singlet oxygen quantum yield,
Zinc phthalocyanine

Abstract: This study aims to demonstrate the synthesis, characterization and the relationship between photochemical and sono-photochemical properties of novel zinc phthalocyanine (**3**) having furan-imine substituent. Both photochemical and sono-photochemical techniques were applied in order to calculate and compare the singlet oxygen quantum yield (Φ_Δ) of the complex (**3**) in DMSO. The singlet oxygen quantum yield of the complex (**3**) was determined as **0.12** by the PDT method (irradiated with only light) ($\Phi_{\Delta PDT}$ = 0.12), while the value of **0.78** was reached by the SPDT approach (combination of light and ultrasound) ($\Phi_{\Delta SPDT}$ = 0.78). Considering the efficiency in singlet oxygen formation, it can be said that the SPDT modality is a more powerful therapeutic solution than the PDT technique and also the complex (**3**) may be a suitable sono-photosensitizer candidate in both PDT and SPDT techniques. This study will also contribute to the field on enhancing singlet oxygen generation by using SPDT approach.

Sono-Fotokimyasal Yöntemle Arttırılmış Singlet Oksijen Oluşumuna Sahip Yeni Furan-İmin Sübstitüeli Çinko Ftalosiyanin

Anahtar kelimeler
Fotodinamik terapi,
Sono-fotodinamik terapi,
Singlet oksijen kuantum verimi,
Çinko ftalosiyanin

Öz: Bu çalışma, furan-imin sübstitüentine sahip yeni çinko ftalosiyaninin (**3**) sentezini, karakterizasyonunu ve fotokimyasal ve sono-fotokimyasal özellikleri arasındaki ilişkiyi göstermeyi amaçlamaktadır. Kompleksin (**3**) DMSO'daki singlet oksijen kuantum verimini (Φ_Δ) hesaplamak ve karşılaştırmak için hem fotokimyasal hem de sono-fotokimyasal teknikler uygulanmıştır. Kompleksin (**3**) singlet oksijen kuantum verimi PDT yöntemi (sadece ışık ışınlaması) ile **0.12** olarak hesaplanmış iken ($\Phi_{\Delta PDT}$ = 0.12), bu değer SPDT yöntemi (ışık ve ultrasonun kombinasyonu) ile **0.78**'e çıkarılmıştır ($\Phi_{\Delta SPDT}$ = 0.78). Singlet oksijen üretim verimliliği göz önüne alındığında, SPDT yönteminin PDT yönteminden daha güçlü bir terapötik yaklaşım olduğu ve ayrıca kompleksin (**3**) hem PDT hem de SPDT uygulamalarında uygun bir sono-fotosensitizer adayı olabileceği söylenebilir. Bu çalışma aynı zamanda, SPDT yöntemini kullanarak singlet oksijen üretimini arttırmaya yönelik alana da katkıda bulunacaktır.

1. Introduction

Photodynamic Therapy (PDT) is a novel modality for treating malignant tumors and it is utilized increasingly nowadays due to its high therapeutic effect and less harmful effect compared to other treatment methods. PDT functions in the existence of light, molecular oxygen, and photosensitizer (light-sensitive substance, PS) [1-3]. In PDT; a combination of three relatively harmless elements is utilized: photosensitizer, light and oxygen, which produce reactive oxygen species (ROS) that are capable of selectively eradicating cancerous cells. In photodynamic therapy, light is used to stimulate the photosensitizer. Therefore, it is indirectly responsible for the formation of singlet oxygen [4-9]. Similarly, the

* Corresponding Author: gurkank@yildiz.edu.tr

treatment method in which ultrasound waves are utilized instead of light to activate the sensitizer (called *sonosensitizer*) is called Sonodynamic Therapy (SDT). SDT was developed as an alternative treatment to PDT and treats tumor with sonosensitizer [10, 11]. SDT is similar to PDT in terms of its low toxicity advantage. The generation of ROS through the combined use of low-intensity ultrasound, molecular oxygen, and a sonosensitizer forms the core mechanism underlying the sonodynamic activity of SDT [12-14]. Compared to PDT, SDT offers the advantage since ultrasound can enter deeper tissues than light, thus offering potential benefits in treating tumors located in less accessible areas [15, 16]. Sono-photodynamic therapy (SPDT), on the other hand, is an innovative and non-invasive therapeutic modality emerging in the field of anticancer that uses combines the strengths of both PDT and SDT [17-19]. The fundamental of this new synergistic approach is the use of both light of a certain wavelength and a specific frequency of sound to activate a light- and sound-sensitive material that selectively binds to tumor cells and causes their lysis. In this way, by enhancing the generation of ROS, SPDT can provide a more effective treatment that targets tumors with increased precision and depth [20-22].
In three therapeutic treatments, the sensitizer is central to the therapeutic mechanism, determining the effectiveness, specificity, and safety of these treatments. Sensitizers must meet a number of physicochemical conditions, including: They must have molar absorption in the phototherapeutic window, high photo/sonostability, and a significant quantum yield of ROS photogeneration [23]. Phthalocyanines (Pcs) fulfill numerous requirements, so photodynamic therapy, sonodynamic therapy, and sono-photodynamic therapy are typically prioritized among the applications of this class of compounds [24-27].

Phthalocyanine compounds, which are important members of the class of the macrocyclic compound, consist of four isoindole segments linked to each other by the nitrogen-binding atom and are planar aromatic structures containing conjugated 18-π electrons [28]. In order for phthalocyanine compounds to have a long triplet life and effective singlet oxygen production, the orbitals of the metal ion they coordinate must be fully filled, i.e. diamagnetic. For this reason, phthalocyanines (Pc) carrying central metal ions such as Si(IV), Ga(III), Zn(II), In(III) and Al(III) are among the preferred sensitizers in PDT [29-32]. Apart from metal ions, halogen-substituted phthalocyanines are also attracting increasing attention due to the enhanced impacts of halogens on the photophysical and photochemical characteristics [33, 34].
Furan and its derivatives are known for their remarkable qualities such as great solvent capabilities, high reactivity and low viscosity. They have found many areas of application for themselves, including in drug synthesis [35], natural materials synthesis [36], and polymer industry [37]. Chemical derivatives of furan groups can also be crucial in modifying the solubility and spectral features of complexes, helping to overcome the solubility issues of phthalocyanines by substituting them in the peripheral and non-peripheral sites of the Pc core [38-40]. Imine (Schiff base) functional group, on the other hand, has a remarkable role in many application areas such as medicine, pharmacy and liquid crystals [41]. Biological activities of imine compounds such as enzyme inhibition, antimicrobial, antioxidant, antiinflammatory and anticancer activities have been extensively studied by researchers. Nevertheless, studies that examine photophysical and photochemical characteristics of phthalocyanines carrying Schiff base segments are very restricted in the literature [34, 42].
In this paper, the synthesis, structural analysis and examination of photophysical and photochemical studies of novel furan-imine substituted zinc phthalocyanine derivative have been presented. The singlet oxygen formation ability of the obtained complex (**3**) has been investigated by both photochemical and sono-photochemical techniques and compared in detail.

2. Material and Method

2.1. Chemicals and instrumentation

The chemicals used in the experimental and measurement stages were commercially supplied by Sigma-Aldrich and were employed directly.
The reactions were tracked by using thin layer chromatography (TLC).
For the FT-IR (ATR) spectra of the compounds, Perkin Elmer Spectrum One Spectrometer was used. ^{1}H-NMR spectra were taken in deuterated dimethyl sulfoxide (DMSO) solution on a Bruker 500 MHz spectrometer. Shimadzu 2001 UV-Vis spectrophotometer was utilized to acquire the absorption spectra of the compounds in the UV-Vis area. In the photo-irradiation calculations, General Electric quartz line lamp (300W) and intor, 670 nm with a bandwidth of 40 nm was used. To measure light intensities, POWER MAX5100 (Mol electron detector incorporated) power meter was employed.

2.2. Synthesis and structural analysis of furan-imine substituted zinc (II) phthalocyanine

The synthesis route for the furan-imine substituted new zinc(II) phthalocyanine is presented in Scheme **1**. At first, the imine intermediate (**1**) was obtained by the reaction between commercially available 5-bromo-2-furaldehyde and 4-hydroxyaniline using glacial acetic acid as a catalyst. Then, compound **2** was synthesized as a result of the etherification reaction between compound **1** and 4-nitrophthalonitrile. In the last stage, with the template effect of phthalonitrile compound **2** and $Zn(CH_3COO)_2$, the

cyclotetramerization reaction under catalytic activity of 1,8-diazabicyclo[5.4.0]undec-7-ene (DBU) was yielded the target compound **3**.

2.2.1. Preparation of compound 1 [(E)-4-(((5-bromofuran-2-yl)methylene)amino)phenol]

A solution of 5-bromofuran-2-carbaldehyde (2.5 mmol) and 4-aminophenol (2.5 mmol) were prepared in ethanol (absolute, 50 mL). The solution was added in a Schlenk tube. As a catalyst, trace amount of acetic acid (glacial) was put in this solution. Then, the reaction mixture was left to stir at 25 °C for one-night. The reaction progress was checked by TLC (Hexane:Ethyl Acetate / 2:1). Upon completion, the mixture was cooled to obtain the yellowish solid to precipitate. Following filtration, the crude product was then collected, washed with hot absolute ethanol, and purified by repeated recrystallization process by using methanol/acetone combination.

Yield: 94 %, 0.62 g. **^{1}H-NMR (500 MHz, DMSO-d6):** δ (ppm) = 9.58 (s, 1 Ar-OH), 8.35 (s, 1H, -CH=N), 7.20 (d, *J* ≈ 8.7 Hz; 2 Ar-H), 7.08 (d, *J* ≈ 3.5 Hz; 1 Ar-H), 6.81 (d, *J* ≈ 3.5 Hz; 1 Ar-H), 6.79 (d, *J* ≈ 8.7 Hz; 2 Ar-H). **MS (HRMS):** *m/z* = Calc. 265.96; Found: 265.98 $[M]^+$.

2.2.2. Preparation of compound 2 [(E)-4-(4-(((5-bromofuran-2-yl)methylene)amino) phenoxy)phthalonitrile]

In a round-bottomed flask, compound **1** (1 mmol) and 4-nitrophthalonitrile (0.9 mmol) were dissolved in Dimethylformamide. The mixture was stirred at room temperature for 20 minutes, and then anhydrous K_2CO_3 (2.7 mmol) was added gradually over a 2 hours period under inert atmosphere.

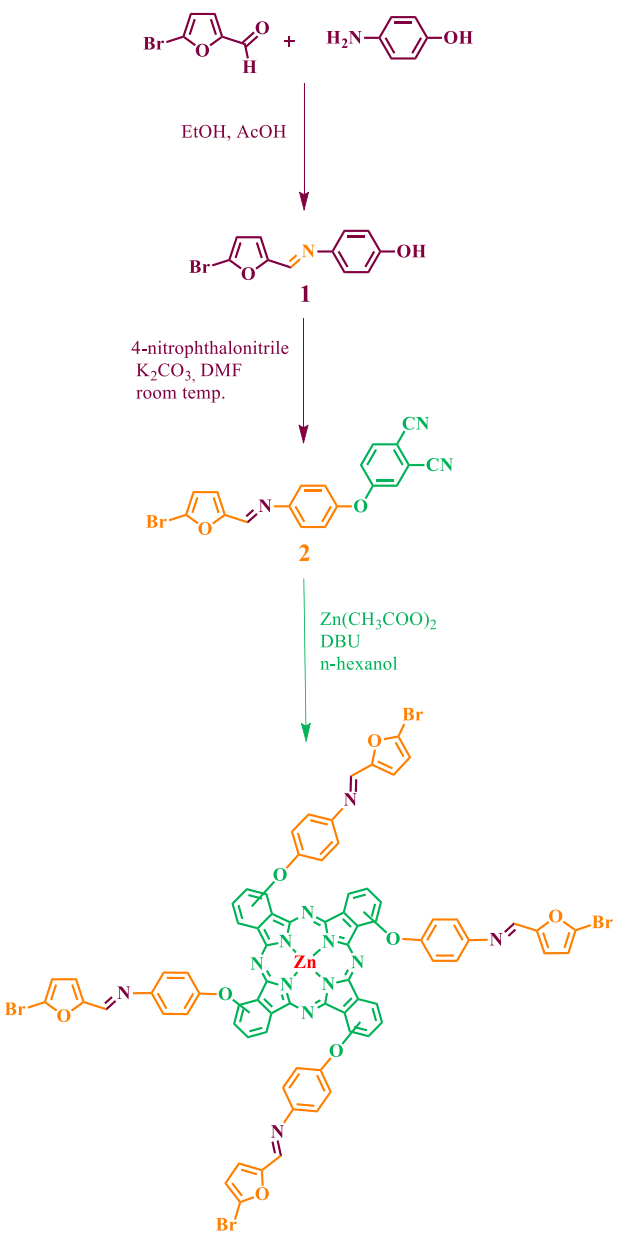

Scheme 1. Synthesis route for furan-imine zinc (II) phthalocyanine (**3**).

After the complete addition of K_2CO_3, the reaction mixture was stirred at room temperature for one night. Once the reaction was finished, the mixture was poured into a 500 mL solution (ice/water). Centrifugation was used to collect the yellowish solid, and it was washed with water until the pH value of filtrate became neutral. After that, hot methanol was used to repeatedly wash the crude product. **Yield:** 70 %, 0.25 g. **^{1}H-NMR (500 MHz, DMSO-d6):** δ (ppm) = 8.42 (s, 1H, -CH=N), 8.12 (d, *J* ≈ 8.7 Hz; 1 Ar-H), 7.82 (s, 1 Ar-H), 7.42-7.40 (m, 3 Ar-H), 7.25 (d, *J* ≈ 8.59 Hz; 2 Ar-H), 7.20 (d, *J* ≈ 3.5 Hz; 1 Ar-H), 6.87 (d, *J* ≈ 3.5 Hz; 1 Ar-H). **FT-IR (ATR):** υ_{max} (cm^{-1}) = 3133.05 (Aromatic C-H), 2230.49 (C≡N), 1631.26 (C=N). **MS (HRMS):** *m/z* = Calc. 392.24; Found: 392.00 $[M]^+$.

2.2.3. Preparation of furan-imine substituted zinc phthalocyanine (3)

A solution of **2** (0.1 mmol) and $Zn(CH_3COO)_2$ (0.1 mmol) was prepared in *n*-hexanol. The solution was mixed under argon atmosphere and a trace quantity of DBU was then put in using a syringe. The reaction mixture was heated to reflux at 130 °C for 4 hours, and the progress was tracked by TLC using THF as solvent. After the reaction was left to room temperature, the green product was collected by adding *n*-hexane, collected via centrifugation process. The purification was achieved by using hot methanol followed by crystallization. Characterization was performed by MS and UV-Vis spectroscopy. **Yield:** 18 %, 0.03 g. **MS (HRMS):** *m/z* = Calc. 1698.37; Found: 1635.17 $[M-Zn+2H]^+$, 1621.08 $[M-Br+3H]^+$, 1570.53 $[M-C_5H_3OBr+Na+8H]^+$, 1531.57 $[M-C_5H_3OBr-8H]^+$.

2.3. Photophysicochemical and sono-photochemical studies

Photophysicochemical and sono-photochemical measurements and the quantum yields obtained from these measurements were carried out following the path presented in [17].

3. Results

3.1. Synthesis and molecular characterization

In the present study, a novel tetra-furan-imine decorated zinc phthalocyanine having heavy atom (Br) was synthesized. Purification of intermediates and the target complex (**3**) has been carried out by recrystallization process. The illumination of chemical structures of all compounds achieved by spectroscopic methods (^{1}H-NMR, FT-IR, MS and UV-Vis). The detailed spectra of the obtained compounds are demonstrated in **Figures 1-6**.

In the ^{1}H-NMR (proton NMR) spectrum of **1** (see **Figure 1**), the peak resonated at 9.58 ppm as singlet belongs to the phenolic O-H. The peak appeared as singlet at 8.35 ppm represents the imine group. Two doublet peaks with the same J value of 8.7 Hz. resonated at 7.20 ppm and 6.79 ppm belong to the phenyl ring and two doublet peaks with the same J value of 3.5 Hz. resonated at 7.08 ppm and 6.81 ppm belong to the furan ring. For the proton NMR spectrum of **2** (see **Figure 3**), protons belonging to the imine segment, furan and phenyl rings resonated at the expected regions. The most apparent evidence of the synthesis of compound **2** is the disappearance of the phenolic proton in the spectrum.

In the FT-IR spectrum of the phthalonitrile derivative **2** (see **Figure 4**), the presence of both C=N vibration in the imine part appeared at 1631.26 cm^{-1} and C≡N vibration in the phthalonitrile unit occurred at 2230.49 cm^{-1} indicates that the compound **2** was successfully synthesized.

The molecular ion peaks of the compounds **1–3** were observed in mass spectra with *m/z* peak at 265.98 $[M]^+$, 392.00 $[M]^+$ and 1635.17 $[M-Zn]^+$, respectively. In addition to $[M-Zn]^+$ for compound **3**; $[M-Br+3H]^+$, $[M-C_5H_3OBr+Na+8H]^+$ and $[M-C_5H_3OBr-8H]^+$ were observed at 1621.08, 1570.53 and 1531.57, respectively (see **Figures 2,5,6**). Considering the mass spectra of the compounds, it can be said that the molecular structures are compatible with the proposed structures.

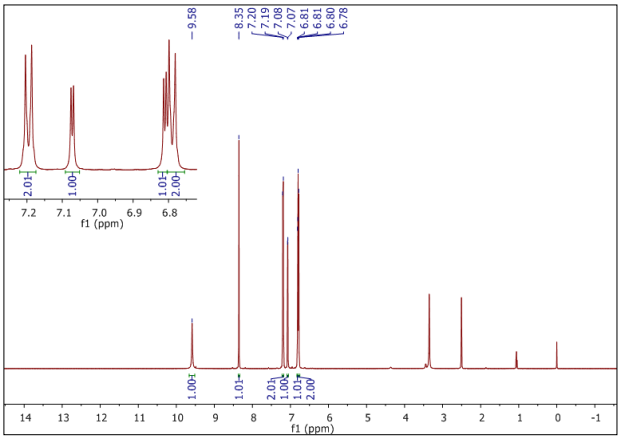

Figure 1. ^{1}H-NMR spectrum of compound **1**.

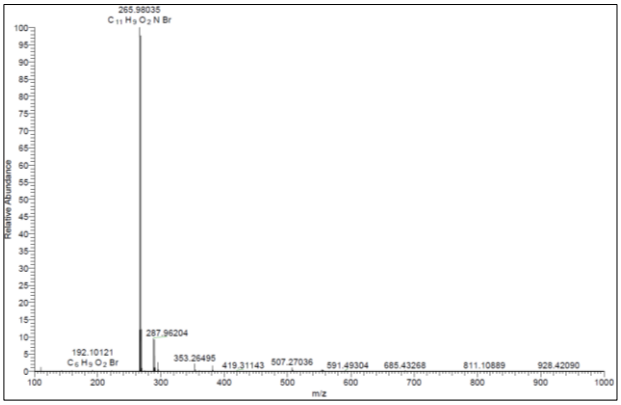

Figure 2. Mass spectrum of compound **1**.

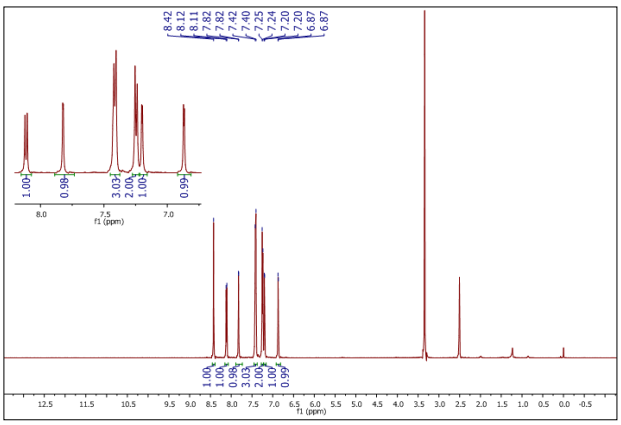

Figure 3. ^{1}H-NMR spectrum of compound **2**.

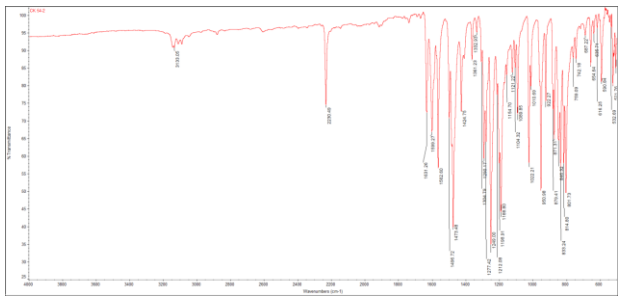

Figure 4. FT-IR (ATR) spectrum of compound **2**.

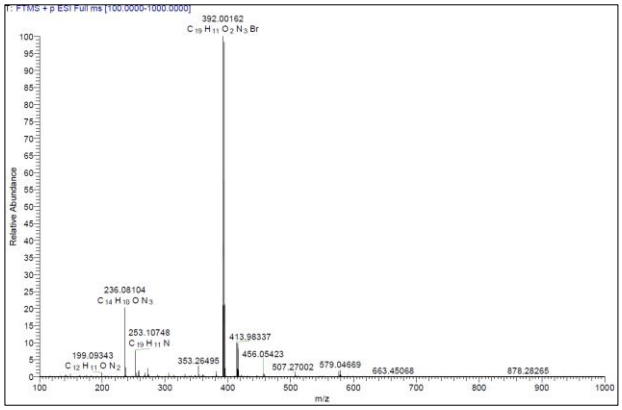

Figure 5. Mass spectrum of compound **2**.

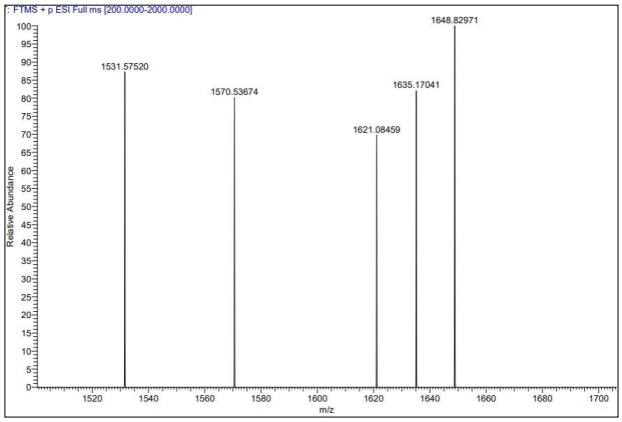

Figure 6. Mass spectrum of compound **3**.

3.2. Photophysical and photochemical studies

3.2.1. Ground state absorption and emission spectra

Phthalocyanine derivatives are characterized by strong Q-band intensities between 600-700 nm and B-band intensities between 250-400 nm. Ground state absorption spectrum of complex **3** was taken in DMSO at room temperature and aggregation study was also carried out in the same solvent. It was seen that compound **3** did not exhibit aggregation. The studies showed that complex **3** obeyed the Lambert-Beer law. The obtained data are presented in **Figure 7** and listed in **Table 1**.

The fluorescence quantum yield (Φ_F) is a crucial metric to evaluate the therapeutic effectiveness of the sensitizer employed in PDT and SPDT. Therefore, understanding and optimizing the Φ_F are a significant aspect of developing effective sono-photosensitizers for PDT and SPDT. To measure emission, a solution of **3** was prepared in DMSO at a concentration of around 9.3×10^{-6} M. The solution was then further diluted and subjected to excitation experiment. **Figure 8** presents the absorption (685 nm), emission (696 nm) and excitation (680 nm) spectra and fluroescence quantum yield is listed in **Table 1**. It can be noted that two spectra, emission and absorption, were identical and also they showed mirror image of fluorescent spectra. The effect of the nature of the segments and the type of the central metal atom on the Φ_F was investigated and the Φ_F was determined as 0.03 in biocompatible solvent, DMSO. The obtained value is lower than the standard zinc phthalocyanine (Φ_F = 0.20) as expected. This diminished fluorescence quantum yield means that the sensitizer translates its energy into some processes such as intersystem crossing rather than being emitted as fluorescence, leading to a more effective generation of reactive oxygen species. Additionally, a Stokes shift of 11 nm was obtained, which is consistent with ZnPc complexes [43].

Table 1. Spectral data of photophysical and sono-photochemical characteristics of **3** in DMSO.

Q-Band λ_{max}, nm	Logε	Emission, λ_{Em}, nm	Excitation λ_{Ex}, nm	Stokes Shift Δ_{Stokes}, nm	Φ_F	$\Phi_{\Delta PDT}$	$\Phi_{\Delta SPDT}$	Φ_d (10^{-3})
685	4.73	696	680	11	0.03	0.12	0.78	0.12

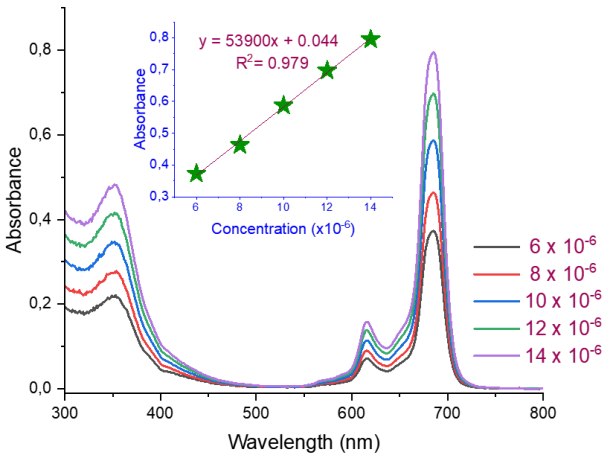

Figure 7. UV-Vis electronic absorption spectrum of complex **3** at increased concentrations in DMSO.

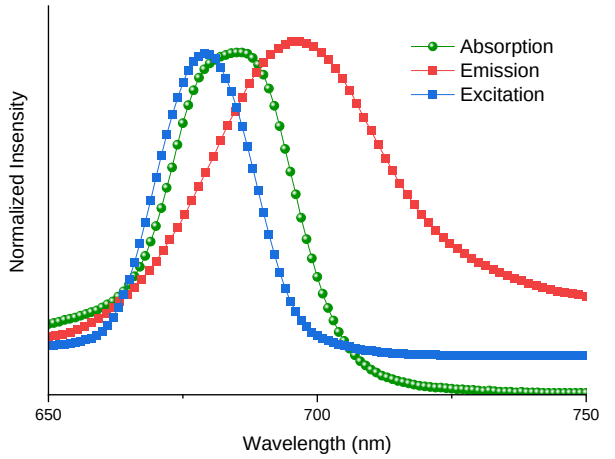

Figure 8. Absorption (685 nm), emission (696 nm) and excitation (680 nm) of complex **3** (9.3×10^{-6} M) in DMSO.

3.2.2. Determination of singlet oxygen formation of both photochemical and sono-photochemical methods

Among the three components in therapeutic applications, singlet oxygen is the most critical one because it is primarily responsible for the damage to malignant tissues and pathogens. Singlet oxygen is produced as one of the ROS by a sensitizer activated by a suitable stimulating element in the existence of sufficient concentrations of $^3O_2$, according to the Type II mechanism. Therefore, the selection of sensitizers that can produce high singlet oxygen is of vital part in the terapeutic treatment methods. In the presented work, in order to measure and reveal the singlet oxygen formation capacity of complex **3**, photodynamic and sono-photodynamic methods were performed. In both processes, unsubstituted ZnPc was used as the standard and 1,3-diphenylisobenzofuran (DPBF) was used as the singlet oxygen trapping-agent. In the photochemical process, after the **3** was dissolved in DMSO and added DPBF, the solution was then triggered with just light (7.05×10^{15} photon s^{-1} cm^{-2} light intensity). On the other hand, ultrasound with 35 kHz, followed by light with 7.05×10^{15} photon s^{-1} cm^{-2} for interval of 5 s were employed in the sono-photochemical method. During the singlet oxygen formation, the change in the absorbance of DPBF at 417 nm was monitored. (see **Figure 9** and **Figure 10**). When it comes to the values of Φ_Δ, it was determined as 0.12 in photochemical method, while 0.78 was found in sono-photochemical measurements (see **Table 1**). The results obtained from the measurements demonstrate that SPDT technique is more powerful than PDT modality in terms of singlet oxygen formation.

Studies have shown that singlet oxygen formation was increased when sono-photochemical method was used [17, 44-46].

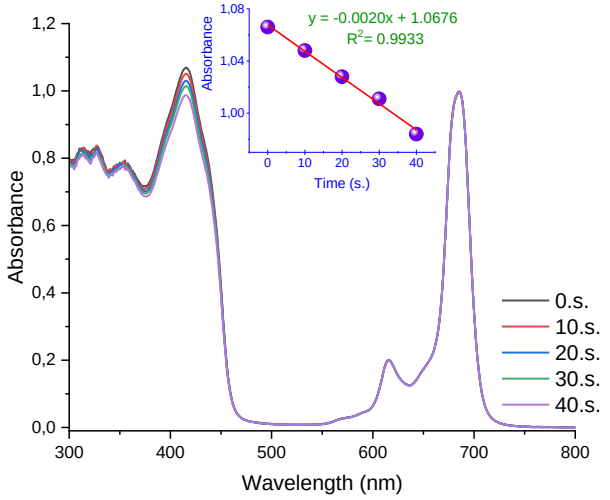

Figure 9. Decrease in DPBF concentrations with photochemical method in complex **3**.

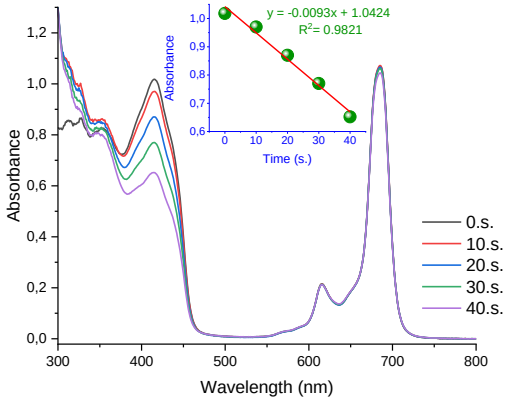

Figure 10. Decrease in DPBF concentrations with sono-photochemical method in complex **3**.

3.2.3. Determination of photostability

Photodegradation quantum yield (Φ_d) has an important place in overall treatment success as it expresses the efficiency with which a photosensitizer undergoes photodegradation when exposed to light. This phenomenon is especially important because it determines how long a photosensitizer is stable under light irradiation. At this stage of the study, the photodurability of complex **3** was determined in

DMSO by exposing to light of intensity of 2.42×10^{16} s^{-1} cm^{-2} at 600-seconds intervals and the change in maximum absorbance in the Q-band was recorded. The photodegradation quantum yield of **3** was calculated as 0.12×10^{-3}. **Figure 11** shows the changes in Q-band intensity during the photodecomposition process of **3**. Studies [1, 47] have shown that the photodecomposition capabilities of Pcs are between 10^{-6} and 10^{-3}. Therefore, it can be said that the photodegradation quantum yield of 0.12×10^{-3} obtained for complex **3** is compatible with the literature and complex **3** is an ideal candidate for PDT and SPDT applications because it remains stable under light exposure and does not undergo decay.

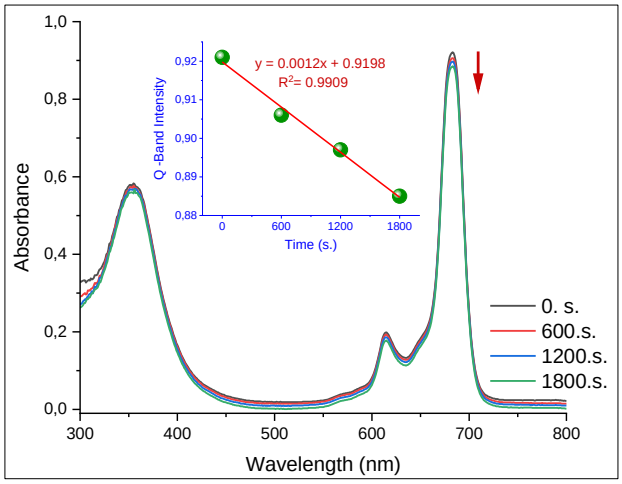

Figure 11. Photodecomposition spectrum of compound **3** (3.7×10^{-5} M) in DMSO.

4. Discussion and Conclusion

As with many other types of macromolecules, the molecular design of the sensitizer in phthalocyanine derivatives plays a paramount role for optimum singlet oxygen production in innovative therapeutic approaches (PDT, SDT and SPDT). It is anticipated that introducing heavy Bromine atom and furan-Schiff base segment along with central zinc metal ion into the same molecule influences both photophysical and sono-photochemical features of the molecule. For this reason, furan-imine zinc (II) phthalocyanine complex (**3**) was derived and its photophysical and sono-photochemical properties examined. Photodecomposition measurements revealed that the compound is stable under light exposure. Moreover, when the singlet oxygen production capacity of the complex **3** was evaluated, Φ_{Δ} value was found to be 0.12 photochemically ($\mathbf{\Phi_{\Delta PDT} = 0.12}$), while this value was increased to 0.78 sono-photochemically ($\mathbf{\Phi_{\Delta SPDT} = 0.78}$). **Figure 12** shows the comparative representation of decrease in DPBF concentration in both methods. The synergistic action of light and ultrasound suggests that the complex **3** may be a potential sono-photosensitizer agent *in vitro* PDT and SPDT studies in the future.

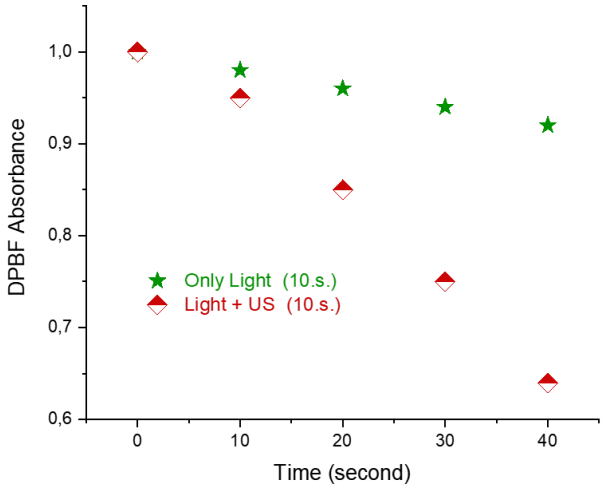

Figure 12. Comparative representation of decrease in DPBF concentration in both methods.

Acknowledgement

I extend my heartfelt gratitude dear Prof. Dr. Ali ERDOĞMUŞ for his endless academic guidance and profound insights.

Declaration of Ethical Code

In this study, we undertake that all the rules required to be followed within the scope of the "Higher Education Institutions Scientific Research and Publication Ethics Directive" are complied with, and that none of the actions stated under the heading "Actions Against Scientific Research and Publication Ethics" are not carried out.

References

[1] Maree SE, Nyokong T. Syntheses and photochemical properties of octasubstituted phthalocyaninato zinc complexes. Journal of Porphyrins and Phthalocyanines. 2001;5(11):782-92.

[2] Nas A, Kahriman N, Kantekin H, Yaylı N, Durmuş M. The synthesis of novel unmetallated and metallated phthalocyanines including (E)-4-(3-cinnamoylphenoxy) groups at the peripheral positions and photophysicochemical properties of their zinc phthalocyanine derivatives. Dyes and Pigments. 2013;99(1):90-8.

[3] Wysocki M, Ziental D, Biyiklioglu Z, Jozkowiak M, Baş H, Dlugaszewska J, et al. Non-peripheral octasubstituted zinc (II) phthalocyanines bearing pyridinepropoxy substituents–Antibacterial, anticancer photodynamic and sonodynamic activity. Journal of Inorganic Biochemistry. 2025;262:112751.

[4] Khoza P, Antunes E, Nyokong T. Synthesis and photophysicochemical properties of zinc phthalocyanine derivatized with benzothiazole

or carbazole photosensitizers. Polyhedron. 2013;61:119-25.

[5] Chen J, Chen Z, Zheng Y, Zhou S, Wang J, Chen N, et al. Substituted zinc phthalocyanine as an antimicrobial photosensitizer for periodontitis treatment. Journal of Porphyrins and Phthalocyanines. 2011;15(04):293-9.

[6] Sağlam Ö, Farajzadeh N, Yaşa Atmaca G, Erdoğmuş A, Koçak MB. Effect of position and connected atom on photophysical and photochemical properties of some fluorinated metallophthalocyanines. Photochemistry and Photobiology. 2021;97(2):270-7.

[7] Al-Raqa SY, Köksoy B, Durmuş M. A novel lutetium (III) acetate phthalocyanine directly substituted with N, N'-dimethylaminophenyl groups via CC bonds and its water-soluble derivative for photodynamic therapy. Tetrahedron letters. 2017;58(7):685-9.

[8] Kwiatkowski S, Knap B, Przystupski D, Saczko J, Kędzierska E, Knap-Czop K, et al. Photodynamic therapy–mechanisms, photosensitizers and combinations. Biomedicine & pharmacotherapy. 2018;106:1098-107.

[9] Atmaca GY, Erdoğmuş A. Synthesis of new water soluble silicon phthalocyanine substituted by linker sulfur atom and photophysicochemical studies for photodynamic therapy. Journal of Porphyrins and Phthalocyanines. 2019;23(11n12):1398-405.

[10] Yumita N, Umemura S-i. Sonodynamic antitumour effect of chloroaluminum phthalocyanine tetrasulfonate on murine solid tumour. Journal of pharmacy and pharmacology. 2004;56(1):85-90.

[11] Wan G-Y, Liu Y, Chen B-W, Liu Y-Y, Wang Y-S, Zhang N. Recent advances of sonodynamic therapy in cancer treatment. Cancer biology & medicine. 2016;13(3):325.

[12] Wang X, Zhong X, Bai L, Xu J, Gong F, Dong Z, et al. Ultrafine titanium monoxide (TiO1+ x) nanorods for enhanced sonodynamic therapy. Journal of the American Chemical Society. 2020;142(14):6527-37.

[13] Huang P, Qian X, Chen Y, Yu L, Lin H, Wang L, et al. Metalloporphyrin-encapsulated biodegradable nanosystems for highly efficient magnetic resonance imaging-guided sonodynamic cancer therapy. Journal of the American Chemical Society. 2017;139(3):1275-84.

[14] Nene LC, Sindelo A, Britton J, Nyokong T. Effect of ultrasonic frequency and power on the sonodynamic therapy activity of cationic Zn (II) phthalocyanines. Journal of Inorganic Biochemistry. 2021;217:111397.

[15] Borah BM, Cacaccio J, Durrani FA, Bshara W, Turowski SG, Spernyak JA, et al. Sonodynamic therapy in combination with photodynamic therapy shows enhanced long-term cure of brain tumor. Scientific Reports. 2020;10(1):21791.

[16] Canavese G, Ancona A, Racca L, Canta M, Dumontel B, Barbaresco F, et al. Nanoparticle-assisted ultrasound: A special focus on sonodynamic therapy against cancer. Chemical Engineering Journal. 2018;340:155-72.

[17] Can Karanlık C, Aguilar-Galindo F, Sobotta L, Guzel E, Erdogmus A. Combination of light and ultrasound: exploring sono–photochemical activities of phthalocyanine-based sensitizers. The Journal of Physical Chemistry C. 2023;127(19):9145-53.

[18] Atmaca GY, Aksel M, Bilgin MD, Erdoğmuş A. Comparison of sonodynamic, photodynamic and sonophotodynamic therapy activity of fluorinated pyridine substituted silicon phthalocyanines on PC3 prostate cancer cell line. Photodiagnosis and photodynamic therapy. 2023;42:103339.

[19] Alves F, Ayala ETP, Pratavieira S. Sonophotodynamic Inactivation: The power of light and ultrasound in the battle against microorganisms. Journal of Photochemistry and Photobiology. 2021;7:100039.

[20] Granados-Tavera K, Zambrano-Angulo M, Montenegro-Pohlhammer N, Atmaca GY, Sobotta L, Güzel E, et al. Synergistic effect of ultrasound and light to efficient singlet oxygen formation for photodynamic purposes. Dyes and Pigments. 2023;210:110986.

[21] Ogbodu RO, Nitzsche B, Ma A, Atilla D, Gürek AG, Höpfner M. Photodynamic therapy of hepatocellular carcinoma using tetra-triethyleneoxysulfonyl zinc phthalocyanine as photosensitizer. Journal of Photochemistry and Photobiology B: Biology. 2020;208:111915.

[22] Atmaca GY, Karanlık CC, Erdoğmuş A. Novel silicon phthalocyanines with improved singlet oxygen generation by Sono-photochemical applications. Journal of Photochemistry and Photobiology A: Chemistry. 2023;436:114365.

[23] Zheng Y, Ye J, Li Z, Chen H, Gao Y. Recent progress in sono-photodynamic cancer therapy: From developed new sensitizers to nanotechnology-based efficacy-enhancing strategies. Acta Pharmaceutica Sinica B. 2021;11(8):2197-219.

[24] Nene LC, Abrahamse H. Design consideration of phthalocyanines as sensitizers for enhanced sono-photodynamic combinatorial therapy of cancer. Acta Pharmaceutica Sinica B. 2024;14(3):1077-97.

[25] Ke M-R, Wang C, He Q, Que R, Wei Y, Zheng B-Y, et al. N-bridging tetra-substituted zinc (II) phthalocyanines with Q-band absorption up to 780 nm and eminent photosensitizing activities for photodynamic therapy. Dyes and Pigments. 2024;227:112169.

[26] Quartarolo AD, Lanzo I, Sicilia E, Russo N. Can phthalocyanines and their substituted α-para-(methoxy) phenyl derivatives act as photosensitizers in photodynamic therapy? A TD-DFT study. Physical Chemistry Chemical Physics. 2009;11(22):4586-92.

[27] Lo P-C, Rodríguez-Morgade MS, Pandey RK, Ng DK, Torres T, Dumoulin F. The unique features and promises of phthalocyanines as advanced photosensitisers for photodynamic therapy of cancer. Chemical Society Reviews. 2020;49(4):1041-56.

[28] Claessens CG, Hahn U, Torres T. Phthalocyanines: From outstanding electronic properties to emerging applications. The Chemical Record. 2008;8(2):75-97.

[29] Roguin LP, Chiarante N, Vior MCG, Marino J. Zinc (II) phthalocyanines as photosensitizers for antitumor photodynamic therapy. The international journal of biochemistry & cell biology. 2019;114:105575.

[30] Karanlık CC, Atmaca GY, Erdoğmuş A. Comparison of singlet oxygen production of ethyl vanillin substituted silicon phthalocyanine using sonophotodynamic and photodynamic methods. Journal of Molecular Structure. 2023;1274:134498.

[31] Burtsev I, Platonova YB, Volov A, Tomilova L. Synthesis, characterization and photochemical properties of novel octakis (p–fluorophenoxy) substituted phthalocyanine and its gallium and indium complexes. Polyhedron. 2020;188:114697.

[32] Calori IR, Tedesco AC. Aluminum chloride phthalocyanine in MCF-7: rationally accounting for state of aggregation of photosensitizers inside cells. Dyes and Pigments. 2020;173:107940.

[33] Oda K, Ogura S-i, Okura I. Preparation of a water-soluble fluorinated zinc phthalocyanine and its effect for photodynamic therapy. Journal of Photochemistry and Photobiology B: Biology. 2000;59(1-3):20-5.

[34] Yüzeroğlu M, Karaoğlan GK, Köse GG, Erdoğmuş A. Synthesis of new zinc phthalocyanines including schiff base and halogen; photophysical, photochemical, and fluorescence quenching studies. Journal of Molecular Structure. 2021;1238:130423.

[35] Roopa D, Shyamsunder K, Karunakar P, Rajabathar JR, Venkatesulu A, Karnan M, et al. Naphtho [2, 1-b] furan derived triazole-pyrimidines as highly potential InhA and Cytochrome c peroxidase inhibitors: synthesis, DFT calculations, drug-likeness profile, molecular docking and dynamic studies. Journal of Molecular Structure. 2023;1287:135685.

[36] Lehner V, Davies HM, Reiser O. Rh (II)-catalyzed cyclopropanation of furans and its application to the total synthesis of natural product derivatives. Organic letters. 2017;19(18):4722-5.

[37] Hithesh MC, Mohana KNS, Harsha YM, Sreelakshmi M, Madhusudhana AM, Kumar MCS. Effects of curing temperature and addition of functionalized graphene oxide on corrosion barrier performance of phenol furfural polymer-amino phenolic resin composite. Progress in Organic Coatings. 2024;188:108164.

[38] Güzel E, Şaki N, Akın M, Nebioğlu M, Şişman İ, Erdoğmuş A, et al. Zinc and chloroindium complexes of furan-2-ylmethoxy substituted phthalocyanines: Preparation and investigation of aggregation, singlet oxygen generation, antioxidant and antimicrobial properties. Synthetic Metals. 2018;245:127-34.

[39] Kahriman N, Ünver Y, Akçay HT, Gülmez AD, Durmuş M, Değirmencioğlu İ. Photophysical and photochemical study on novel axially chalcone substituted silicon (IV) phthalocyanines. Journal of Molecular Structure. 2020;1200:127132.

[40] Yarasir MN, Kandaz M, Güney O, Salih B. Synthesis and photophysical properties of metallophthalocyanines substituted with a benzofuran based fluoroprobe. Spectrochimica Acta Part A: Molecular and Biomolecular Spectroscopy. 2012;93:379-83.

[41] Karanlık G, Ocak H, Eran BB. Imine based chiral liquid crystals: effect of varying the terminal substituent and orientation of ester linking unit. Journal of Molecular Liquids. 2019;275:567-77.

[42] Harmandar K, Saglam MF, Sengul IF, Ekineker G, Balcik-Ercin P, Göksel M, et al. Novel triazole containing zinc (II) phthalocyanine Schiff bases: Determination of photophysical and photochemical properties for photodynamic cancer therapy. Inorganica Chimica Acta. 2021;519:120286.

[43] Senge MO, Renner MW, Kallisch WW, Fajer J. Molecular structure of (5, 10, 15, 20-tetrabutyl-2, 3, 7, 8, 12, 13, 17, 18-octaethylporphyrinato) nickel (II)—correlation of nonplanarity with frontier orbital shifts. Journal of the Chemical Society, Dalton Transactions. 2000(3):381-5.

[44] Ünlü S, Elmalı FT, Atmaca GY, Erdoğmuş A. Synthesis of phenanthroline substituted five-nuclear phthalocyanine zinc complex and exploring of photochemical and sono-

photochemical properties. Polyhedron. 2024;250:116817.

[45] Aydogdu S, Atmaca GY, Erdoğmuş A, Hatipoglu A. Synthesis of a new Zn-phthalocyanine, photophysical, photochemical, and sono-photochemical properties and DFT studies. Polyhedron. 2024;256:116989.

[46] Köse GG, Erdoğmuş A. Dual effect of light and ultrasound for efficient singlet oxygen generation with novel diaxial silicon phthalocyanine sensitizer. Photochemistry and Photobiology. 2024;100(1):52-66.

[47] Nyokong T. Effects of substituents on the photochemical and photophysical properties of main group metal phthalocyanines. Coordination Chemistry Reviews. 2007;251(13-14):1707-22.